

Kelco Microbial Polysaccharides S-130 (Welan) and S-657 Display Similar Dilute Aqueous Solution Behavior

Ranieri Urbani & David A Brant*

Department of Chemistry, University of California, Irvine, California 92717, USA

(Received 12 September 1988, accepted 25 November 1988)

ABSTRACT

The comb-like, branched microbial polysaccharides S-130 (welan gum) from Alcaligenes ATCC 31555 and S-657 from Xanthomonas ATCC 53159, produced by the Kelco Division of Merck, have potential commercial applications as non-gelling water-soluble thickening and suspending agents. Each is structurally related to the Kelco linear copolysaccharide S-60 (gellan gum) from Auromonas ATCC 31461 which forms gels in aqueous salt solutions and has the repeating unit structure $[\rightarrow 3)\text{-}\beta\text{-D-Glcp}\text{-}(1\rightarrow 4)\text{-}\beta\text{-D-GlcpA}\text{-}(1\rightarrow 4)\text{-}\beta\text{-D-Glcp}\text{-}(1\rightarrow 4)\text{-}\alpha\text{-L-Rhap}\text{-}(1\rightarrow]$. In S-130 this backbone is regularly glycosylated at C(3) of the second $\beta\text{-D-Glcp}$ with $\alpha\text{-L-Rhap}$ (67%) or $\alpha\text{-L-Manp}$ (33%), while in S-657 regular glycosylation occurs at the same backbone site with $\alpha\text{-L-Rhap}\text{-}(1\rightarrow 4)\text{-}\alpha\text{-L-Rhap}$. Both S-130 and S-657 were purified, degraded to various extents by sonication and, for most samples, fractionally precipitated into moderately dispersed fractions differing in mean molecular weight.

Potentiometric proton titration and investigations of the dependence of intrinsic viscosity on ionic strength suggest only very weak polyelectrolyte behavior. For neither polymer does the temperature or ionic strength dependence of optical activity or reduced specific viscosity present evidence of a conformational change in the temperature range $20\leq T\leq 62^\circ\text{C}$. Light scattering as a function of ionic strength discloses a modest tendency of both polymers to aggregate with increasing aqueous NaCl concentration in the range 0.001-0.100 M, intrinsic viscosities were large relative to the molecular weights and essentially constant over the same range of salt concentration. The mean chain extension per backbone sugar residue measured by light scattering, as well as the molecular weight dependence of the intrinsic viscosity, suggest a highly extended

*To whom correspondence should be addressed

chain configuration, similar for the two polymers and comparable to that of the most highly extended cellulose derivatives. This is found despite the periodic occurrence in S-130 and S-657 of the α -(1→3)-linkage, which is expected on elementary grounds to disrupt the essentially rectilinear propagation of the otherwise cellulose-like backbone and generate a less extended chain configuration

INTRODUCTION

Polymers of the Kelco gellan family (Moorhouse, 1987) present an attractive opportunity for studying the influence of comb-like branching on the solution properties of bacterial polysaccharides. Gellan (S-60), the regularly repeating polymer of the unbranched tetrasaccharide ABCD shown in Fig 1, forms sturdy and potentially useful aqueous gels at modest polymer concentration in the presence of various low molecular weight salts (Sanderson, in press, Grasdalen & Smidsrød, 1987). This property may reflect a propensity of aqueous gellan chains to dimerize, revealed in X-ray diffraction studies of partially crystalline cast and stretched gellan films (Chandrasekaran *et al* , 1988). A family of polymers related to gellan through glycosylation of the repeating backbone tetramer does not gel but conveys to its aqueous solutions instead a significant viscosity increment per unit mass of dissolved polysaccharide with or without added low molecular weight salt. The com-

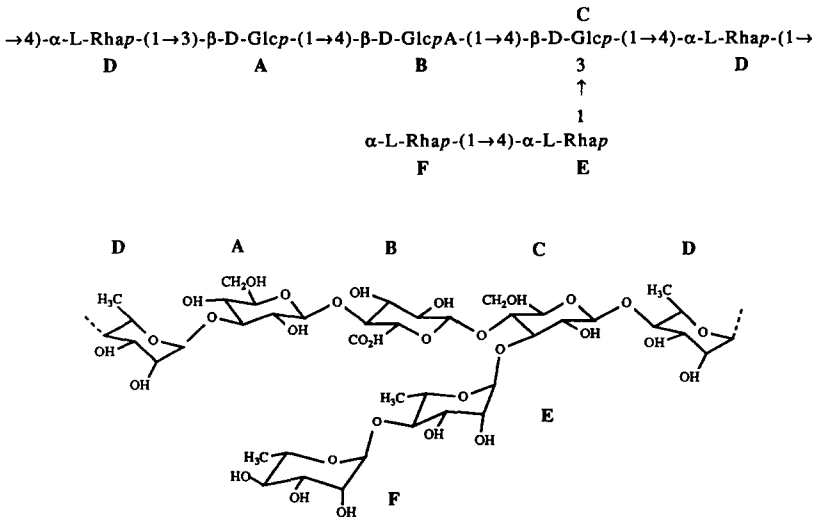


Fig. 1. A schematic drawing of the gellan backbone repeating unit ABCD with the S-130 side chain E (drawn here exclusively as α -L-Rhap but in fact occurring one-third of the time as α -L-Manp) and the S-657 side chain EF attached

parative aqueous solution behavior of these structurally related polysaccharides has recently been reviewed by Moorhouse (1987), and reports of efforts to correlate the dilute solution behavior of the gellan family with differences in their chemical structures have begun to appear (Brownsey *et al*, 1984, Crescenzi *et al*, 1986, 1987, Grasdalen & Smidsrød, 1987, Talashek & Brant, 1987). The present study compares the dilute solution properties of Kelco polymers S-130 (welan) produced by a strain of *Alcaligenes* (ATCC 31555) and S-657 from a *Xanthomonas* (ATCC 53159). The close structural relationship of S-130 and S-657 to one another and to the unbranched S-60 is shown in Fig. 1. Previous studies of S-130 have been reported by Crescenzi *et al* (1986, 1987) and by Talashek & Brant (1987), the dilute solution behavior of S-657 has not previously been described. Weak dependence of the intrinsic viscosity of S-130 on salt concentration and its calorimetric behavior suggest (Crescenzi *et al*, 1987) that the carboxylic acid functionality of the backbone glucuronic acid (residue B) in S-130 is screened, perhaps through interaction with side chain residue E, so as to diminish the polyelectrolyte character of the polymer. Comparative conformational analysis of S-130 and S-60 did not disclose the origin of this putative effect in the van der Waals interactions of backbone and side chain (Talashek & Brant, 1987).

EXPERIMENTAL

Sample preparation

The partially purified polymers were supplied by R. Moorhouse of the Kelco Division of Merck and Company, San Diego, and were treated identically. The powdered polymer (*c.* 1.7 g) was dissolved in 1 liter of distilled water containing 0.1 M NaCl and 0.02% NaN₃ (antimicrobial agent) with vigorous stirring for 2 h. The resulting turbid solutions were sonicated at full power with cooling in an ice bath using a Heat Systems Sonicator (375 W, 20 kHz) with a 12.7 mm diameter titanium horn tip. Four samples of each polymer, designated 130-0.5, 130-1, 130-2, 130-4, 657-0.5, 657-1, 657-2 and 657-4, were prepared by sonicating for 0.5, 1, 2 and 4 h, respectively. The sonicated solutions were centrifuged for 2 h at 12 000 rpm (Sorvall RC2-B, GS-3 rotor), filtered through 1.5 μ m or 3.0 μ m Millipore filters, and the polymer precipitated with 2-propanol, recovered by centrifugation and redissolved in distilled water. Each of the resulting solutions was separated into three fractions by fractional precipitation with 2-propanol as follows:

The precipitant was added gradually to the polymer solution at 23°C with magnetic stirring. Once permanent turbidity had been achieved, the solution was heated to 35°C. After 3 h at 35°C the solution was allowed to cool overnight to 23°C, and the precipitated fraction was collected by centrifugation. The middle fractions, consisting typically of one-third of the original material, were retained for the viscometric and light-scattering experiments reported here. These were redissolved in distilled water, dialyzed for three days against 0.01 M EDTA (Na⁺ salt) containing a small amount of NaCl, and finally dialyzed exhaustively against Milli-pore Milli-Q water until the dialyzate showed no trace of Cl⁻ as judged by addition of AgNO₃. These salt-free solutions of the polymer, presumed to be in the Na⁺ salt form, were concentrated if necessary by rotary evaporation to *c* 1 liter, and the polymer concentration was determined by evaporation to constant weight (at 60°C, 1 mm Hg) of 10 ml aliquots.

These salt-free stock solutions, containing 0.04–0.06% polymer by weight, were stored at 2°C and used to prepare solutions for viscometric and light-scattering experiments, reported below, by the addition of measured amounts of crystalline NaCl (or other cosolutes) to measured aliquots of the stock solution and dilution with Milli-Q water to achieve the desired concentrations of polymer and cosolute. Potentiometric, chiroptical and some of the viscometric experiments reported below were carried out using polymer samples sonicated for 0.5 h and processed identically but without fractional precipitation. The concentrations of the salt-free polymer stock solutions were generally low enough so that even when used undiluted in light-scattering or intrinsic viscosity ($[\eta]$) measurements they had polymer concentrations below the critical overlap concentration c_2^* given approximately by $[\eta]^{-1}$.

Potentiometric proton titrations

The polymer was converted to the fully protonated form by dialyzing an aliquot of the salt-free stock solution for five days against 0.01 M acetic acid, or by passing a portion of the stock solution through a strong cation exchange resin in the protonated form (Fisher Rexyn 101 (H)). Resulting solutions were dialyzed exhaustively against Milli-Q water, and concentrations were determined as above by dry-weight analysis. The two procedures yielded essentially identical titration curves. Titrations were performed on 10 or 20 ml of *c* 0.075% polymer solution, freed of CO₂ by bubbling N₂ and maintained under an N₂ atmosphere, using a Hamilton precision 10 μl syringe to deliver the titrant (0.1000 M NaOH, Fisher). Measurement of pH was carried out in a thermostated vessel

(25°C) with a Kruger and Eckels Model 113 pH meter and a Broadley and James combination calomel-glass electrode calibrated with standard buffers at pH 4 and 10. Data were converted to plots of logarithmic apparent acid dissociation constant, pK_a , versus degree of dissociation, α , using methods described previously (Dubin & Brant, 1975), required blank titrations were performed on Milli-Q water.

Optical activity measurements

Specific optical activity at wavelength λ , defined as

$$[\alpha]_{\lambda} = \alpha/dc_2$$

where α is the observed rotation in degrees, d is the cell pathlength in dm, and c_2 is the polymer concentration in g/ml, was measured on solutions of S-130 and S-657 containing NaCl and other cosolutes using a Perkin-Elmer 241 MC spectropolarimeter. Measurements of $[\alpha]_{\lambda}$ as a function of temperature and cosolute concentration were made using a jacketed polarimeter cell attached to a circulating thermostat bath.

Viscosity measurements

Intrinsic viscosities were measured using Cannon-Ubbelohde Size 50 suspended level capillary viscometers thermostated to $\pm 0.05^\circ\text{C}$ as reported earlier (Buliga & Brant, 1987). Flow times were long enough to obviate kinetic energy corrections, no attempt was made to deduce the possible dependence of the results on shear rate. Flow times were measured initially on polymer solutions prepared from the salt-free stock solutions as described above under Sample preparation. These were subsequently diluted in the viscometer with Milli-Q water containing concentrations of NaCl identical to those in the initial polymer solutions.

Light scattering

Total intensity (integrated) light-scattering measurements were conducted using a Brookhaven Instruments BI-200SM goniometer with a Lexel Model 85 argon ion laser as incident source. Scattered photons were detected over the angular range $30\text{--}150^\circ$ with an EMI-9865A photo-multiplier, and total counts per counting period were recorded at each angle and polymer concentration in Channel A of a Brookhaven BI-2030 correlator. The mean number of counts per counting period, averaged over 5 to 10 successive counting periods, was always used at

each angle and polymer concentration. The laser was tuned to the 488 nm blue-violet line and a power of *c.* 70 mW was typically employed. Data were processed with the microcomputer associated with the Brookhaven instrument using equations given previously (Hacche *et al.*, 1987), altered only to account for the vertically polarized character of the incident radiation, i.e. K given in eqn (2) of Hacche *et al.* (1987) was multiplied by a factor of 2 and the $\cos^2\Theta$ term in the denominator of α in eqn (3) was omitted.

The incident laser intensity was monitored periodically by measuring the scattering from pure benzene at $\Theta = 90^\circ$, $i_B(90)$. The latter quantity enters K along with the Rayleigh ratio of benzene, $R_B = 35.4 \times 10^{-6} \text{ cm}^{-1}$ (Bender *et al.*, 1986) to express the incident light intensity needed to formulate the Rayleigh ratio of the polymer (Goebel & Brant, 1970). The differential refractive index increment was approximated as 0.144 ml/g (Hacche *et al.*, 1987). Linear least squares fits to both the angular and concentration dependences in the Zimm plot of the scattering data were employed. Instrument alignment was confirmed and, if necessary, adjusted at least daily by measuring the angular dependence of the scattering from pure benzene, the function

$$100[(i_B(\Theta) \sin \Theta / \langle i_B(\Theta) \sin \Theta \rangle) - 1]$$

where the angle brackets imply the average over all angles, was required to be ≤ 1.5 to satisfy the alignment criterion. Solutions were prepared for scattering as described under Sample preparation. These were delivered by syringe through the Parafilm cover of a carefully cleaned scattering cell. Millipore filters with pore sizes 0.45 and 0.22 μm , mounted in series on the syringe, were used to clarify the solutions. Minimal sample contamination due to dust was encountered. Extraneous scattering due to any residual dust in the sample was minimized by eliminating the data from any counting period that differed by more than 1.5% from the mean over several successive counting periods at a given angle and polymer concentration. Scattering cells were 12 \times 75 mm Fisher cylindrical borosilicate disposable glass culture tubes selected for proper diameter to match the cell holder and for freedom from obvious optical flaws. Filled cells were suspended in the goniometer with toluene as the thermostating and index matching fluid and rotated to select entrance and exit 'windows' for the incident beam, which minimized the visually detectable stray light arising from the glass or from the poorly index-matched glass-water interfaces. The most concentrated polymer solutions were usually *c.* 0.05%, the least concentrated solutions typically displayed scattering intensities 3–5 times that of the solvent.

RESULTS AND DISCUSSION

Unfractionated polymers

Unfractionated samples of S-130 and S-657 were used to investigate the possibility of a conformational change induced by changes in degree of ionization, temperature and low molecular weight salt concentration. The respective samples of S-130 and S-657 were found by light scattering to have weight-average molecular weights \bar{M}_w of $6.8 \pm 0.7 \times 10^5$ and $9 \pm 1 \times 10^5$ g/mol

Potentiometric titrations

Potentiometric titration data for both polymers dissolved in salt-free aqueous solution appeared reproducibly as straight, horizontal lines when plotted in the conventional format (pK_a versus α), indicating that the ease of carboxyl proton removal from the polymeric glucuronic acid residues is independent of the degree of ionization. Throughout the entire titration range $0.35 \leq \alpha \leq 1$ ($3.4 \leq \text{pH} \leq 10.5$) pK_a for S-130 was constant at 3.7 ± 0.1 . Similarly, for S-657, $pK_a = 3.9 \pm 0.1$ for $0.35 \leq \alpha \leq 1$ ($3.6 \leq \text{pH} \leq 10.5$). This behavior is unusual for a polycarboxylic acid, especially in the absence of screening of the polymeric charge by low molecular weight electrolyte. It suggests that the carboxyl groups are spaced far enough apart so that there is no electrostatic interaction between them or that the expansion of the polymer in response to increasing mean linear charge density (proportional to α) is just sufficient at all α to render constant the mean volume density of charge which governs pK_a (Dubin & Brant, 1975). The alternative possibility that some of the carboxyl groups are buried, and consequently are not titratable at pH 10.5, seems quite remote, especially in the absence of any evidence adduced here for ordered structure in either polymer. The latter finding would also appear to rule out an explanation of the pK_a versus α behavior on the basis of a cooperative charge-induced conformation change (Dubin & Brant, 1975).

Unusual titration behavior is sometimes associated with aggregation and incipient precipitation of the weakly charged polyion at low α (Cesàro *et al.*, 1987), although some evidence of minor salt-induced aggregation is reported below, none of the turbidity at low α usually associated with this behavior was observed. It is noteworthy that the equivalent weights determined for S-130 and S-657 from the titration experiments were 1186 ± 173 and 1726 ± 14 g/equivalent, respectively. These suggest considerably greater spacing of carboxyl groups along the

chain backbone than the $c \approx 20 \text{ \AA}$ associated with the nominal equivalent weights 797 and 938 g/equivalent which are dictated by the published structures in Fig 1 (Jansson *et al.* 1985, O'Neill *et al.*, 1986, Chowdhury *et al.*, 1987) if the naturally occurring acyl content of the polymers is ignored (not shown in Fig. 1).

Optical activity measurements

Crescenzi *et al.* (1986, 1987) report that for S-130, in contrast to S-60, $[\alpha]_{302}$ is essentially independent of T over the range 10–70°C and independent of ionic strength in the presence of the salts Me_4NCl and $\text{Ca}(\text{ClO}_4)_2$. This behavior of S-130 is confirmed with the present unfractionated sample in a wider range of salts, and similar results are found for S-657, as shown in Fig. 2, where only in aqueous 60% DMSO does $[\alpha]_{436}$ deviate significantly from -170 ± 5 over the temperature range 20–62°C

Intrinsic viscosity measurements

For neither S-130 nor S-657 does η_{sp}/c_2 show any unusual temperature dependence at $c_2 = 0.03 \text{ g/dl}$ in aqueous 0.1 M NaCl (Fig 3). Note that the observed magnitude of η_{sp}/c_2 betokens a rather large chain extension for polymers with the molecular weights in question, and a dependence of η_{sp}/c_2 on shear rate may be anticipated. As a function of added NaCl concentration, c_s , the intrinsic viscosity, $[\eta]$, varies linearly with $c_s^{-1/2}$ as is typical for ionic polysaccharides and other polyelectrolytes (Smidsrød

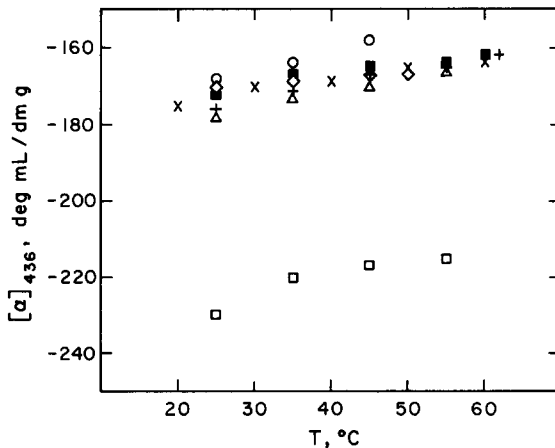


Fig. 2. Plot of $[\alpha]_{436}$ for unfractionated S-657 versus temperature in pure water (\circ) and in various aqueous solvents containing 0.1 M NaCl (\times), 0.1 M CaCl_2 (\diamond), 0.05 M CaCl_2 (\blacksquare), 60% DMSO (\square), 1 M urea ($+$) and 6 M urea (\triangle)

& Haug, 1971). This behavior is shown in Fig 4, where the point obtained at the lowest $c_1 (5 \times 10^{-5} \text{ M})$ in fitting the data for S-657 is arbitrarily ignored, despite the absence of any significant deviation from linearity at low c_2 in the plot of η_{sp}/c_2 versus c_2 . Indeed, only when pure H_2O was used as solvent, did the authors observe for either polymer the upturn in this plot usually observed at low c_2 for aqueous polyelectrolytes

Crescenzi *et al* (1987) reported no change in $[\eta]$ with c_1 for S-130 in aqueous Me_4NCl in the range $0.008 \leq c_1 \leq 0.150 \text{ M}$ ($11.18 \geq c_1^{-1/2} \geq 2.58$), and this conclusion is not inconsistent with the present data in aqueous NaCl in this range of c_1 , given the experimental uncertainty of $\pm 0.1 \text{ dl/g}$ of the $[\eta]$ values. When still smaller values of c_1 are investigated in aqueous NaCl , a weak dependence of $[\eta]$ on c_1 is disclosed for both polymers (Fig 4). The slope $S \approx 0.075$ of the plots of $[\eta]$ versus $c_1^{-1/2}$ in Fig 4 is, however, very much smaller than that observed for many other polyelectrolytes, including several ionic polysaccharides usually

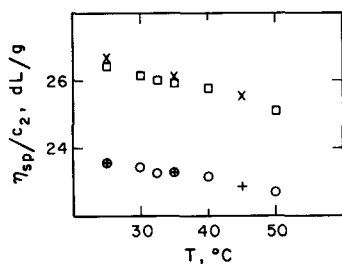


Fig. 3 Plots of η_{sp}/c_2 versus temperature for unfractionated S-130 (○, +) and S-657 (□, ×) in aqueous 0.1 M NaCl at $c_2 = 0.03 \text{ g/dl}$. Open symbols for ascending temperature, crosses and plus signs for descending temperature

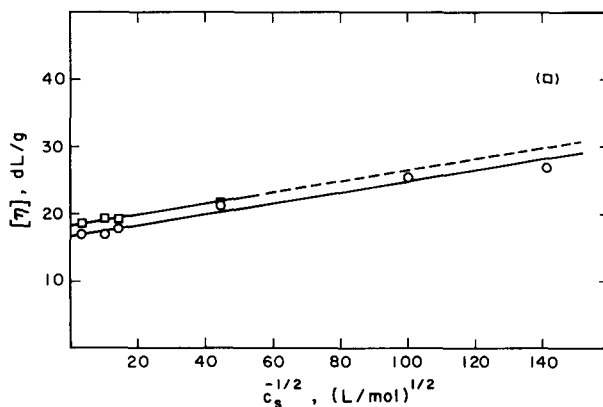


Fig. 4. Plots of $[\eta]$ versus $c_1^{-1/2}$ for unfractionated S-130 (○) and S-657 (□) with linear least squares regression lines, the line through the S-657 data ignores the point at the smallest c_1 .

described as 'stiff', having comparable 'high salt', i.e. $c_s = 0.1$ M, intrinsic viscosities $[\eta]_{0.1}$ (Smidsrød & Haug, 1971). For example, $S \approx 2$ for sodium alginate samples with $[\eta]_{0.1} \approx 18$ dl/g (Smidsrød & Haug, 1971), while for S-194, another member of the Kelco gellan family of ionic polysaccharides, $S \approx 0.9$ with a value of $[\eta]_{0.1} \approx 11$ dl/g (Crescenzi *et al.*, 1987). Even if the previously ignored value of $[\eta]$ for S-657 at $c_s = 5 \times 10^{-5}$ M is taken into account, S for this polymer increases to only 0.16.

Using intrinsic viscosity data for the polymer fractions reported below, it is deduced that the Smidsrød & Haug (1971) characteristic parameter $B \approx 0.03$ for S-130 and S-657. Interpreted strictly as a stiffness parameter, this value of B implies that S-130 and S-657 are stiffer than any of the ionic polysaccharides investigated by Smidsrød & Haug (1971), including carboxymethyl cellulose, sodium alginate and sodium pectinate. Given the results of the potentiometric titrations of S-130 and S-657, however, the small value of B is probably best interpreted in terms of a very weak polyelectrolyte character for S-130 and S-657. Smidsrød & Haug (1971) demonstrated for highly esterified samples of sodium pectinate, with equivalent weights comparable to those measured here for S-130 and S-657, that B can take values of 0.03 and less, presumably because of the diminished polyelectrolyte character of these chains. Further reason to mistrust B as a stiffness parameter in the present case are the values 0.02–0.03 observed for the exponent ν in the equation $S = B([\eta]_{0.1})^\nu$. In all cases investigated by Smidsrød & Haug (1971), for which a correlation of B and other measures of chain stiffness was demonstrated, $\nu \geq 1.2$.

Fractionated samples

The characteristics of four fractions each of S-130 and S-657 as determined by light scattering and viscosity in the range of NaCl concentration $0.001 \leq c_s \leq 0.100$ M are given in Tables 1 and 2, respectively. Weight-average molecular weights, root mean square z -average radii of gyration ($\langle s^2 \rangle_z^{1/2}$), light-scattering osmotic second virial coefficients (A'_2), intrinsic viscosities and Huggins' constants (k') are reported. Quantities in parentheses in Tables 1 and 2 are the standard deviations of the reported quantities for cases where multiple determinations have been carried out. The number of multiple determinations is displayed in square brackets next to the reported \bar{M}_w values, these bracketed numbers are omitted from the corresponding $\langle s^2 \rangle_z^{1/2}$ and A'_2 values reported later in the tables. Absence of parenthetical or bracketed quantities adjacent to any entry in Table 1 and 2 implies that only a single measurement was

TABLE 1
Measured Characteristics of S-130 Fractions

	<i>NaCl concentration (M)</i>			
	<i>0.001</i>	<i>0.005</i>	<i>0.01</i>	<i>0.1</i>
$10^{-3} \bar{M}_w, \text{g/mol}$	283(19)[2] 263(49)[2] 203(7)[2] 158(6)[2]	322(48)[2] 279[1] 236(6)[2] 179(4)[2]	322(22)[2] 226(9)[2] 211(6)[2] 143(6)[2]	359(51)[2] 256(18)[2] 202(7)[2] 140(2)[2]
$\langle s^2 \rangle_c^{1/2}, \text{nm}$	69.4(1.3) 73.5(8.1) 58.1(3.4) 44.3(1.6)	80.5(5.5) 83.1 77.1(8.6) 56.4(0.6)	85.9(8.7) 78.4(1.4) 72.8(4.7) 54.8(3.2)	107.7(13.5) 88.4(3.3) 80.7(0.5) 57.6(1.8)
$10^3 A'_2, \text{ml mol/g}^2$	16.1(1.1) 21.0(3.0) 6.8(0.7) 4.8(2.1)	7.3(2.0) 9.0 5.8(1.6) 4.0(0.6)	5.1(0.5) 5.1(1.6) 4.4(1.3) 1.4(0.8)	1.9(0.3) 1.6(0.3) 1.5(0.4) 1.2(0.1)
$10^2 \langle s^2 \rangle_c / \bar{M}_w, \text{nm}^2 \text{mol/g}$	1.7 2.1 1.7 1.2	2.0 2.5 2.5 1.8	2.3 2.7 2.5 2.1	3.2 3.1 3.2 2.4
$[\eta], \text{dl/g}$	24.71 15.37 10.78 7.38	23.84 15.10 9.81 6.43	23.70 — — —	23.70 15.10 9.84 6.41
k'	0.863 0.999 0.987 0.944	0.632 0.638 0.733 0.651	0.621 — — —	0.621 0.513 0.551 0.460

Quantities in parentheses are the standard deviations for cases where multiple determinations have been carried out

Quantities in square brackets are the number of multiple determinations

Absence of parenthetic or bracketed quantities implies that only a single measurement was made

made. Within each group of reported quantities, the entries for the samples sonicated least (0.5 h) are presented first, and subsequent entries correspond to progressively longer sonication times

Dependence on added salt concentration

Plots of \bar{M}_w versus $\log c_s$ are given in Figs 5 and 6 for S-130 and S-657, respectively. The molecular weights of all fractions are independent of c_s

TABLE 2
Measured Characteristics of S-657 Fractions

	NaCl concentration (M)					
	0.001	0.002	0.005	0.01	0.03	0.1
$10^{-3} \bar{M}_w$, g/mol	440[1] 340(34)[3] 227(17)[2] 224[1]	538[1] 487[1] 263[1] 246[1]	676[1] 364(51)[2] 247(16)[2] 222(19)[3]	799(83)[2] 352(85)[2] 229(4)[2] 237(27)[2]	1085[1] 398[1] 220[1] 243[1]	856(142)[4] 412[1] 218(30)[2] 253(4)[2]
$(s^2)^{1/2}$, nm	85.0 89.6(7.4) 70.8(6.0) 44.7	102.4 117.2 85.1 70.9	141.2 97.5(1.0) 76.0(8.5) 62.3(7.3)	144.0(3.0) 99.1(3.0) 72.6(6.0) 69.2(5.8)	154.2 108.0 71.6 77.9	154.0(8.0) 114.0 74.5(5.0) 72.0(12.0)
$10^3 A'_2$, ml mol/g ²	1.1 8.6(0.7) 20.3(0.3) 5.8	2.9 6.5 14.6 8.7	2.2 3.5(0.2) 7.1(0.2) 3.6(0.7)	2.1(0.1) 2.6(0.7) 4.4(0.3) 3.0(0.7)	1.7 1.2 1.9 2.0	1.5(0.7) 1.9 0.9(0.2) 1.1(0.4)
$10^2 (s^2)_z / \bar{M}_w$, nm ² mol/g	1.6 2.4 2.2 0.9	1.9 2.8 2.8 2.0	2.9 2.6 2.3 1.6	2.6 2.8 2.3 2.0	2.2 2.9 2.3 2.5	2.8 3.2 2.5 2.0
$[\eta]$, dl/g	21.94 14.52 7.52 8.38	— — — —	21.43 13.80 6.80 7.55	21.43 — — —	— — — —	20.97 13.80 6.80 7.50
k'	0.810 0.728 0.986 0.620	— — — —	0.631 0.585 0.703 0.479	0.631 — — —	— — — —	0.595 0.585 0.703 0.428

For meaning of parentheses and brackets, see foot of Table 1

within the experimental uncertainty of the measurements, except for those of the least degraded fractions, 130-0.5 and 657-0.5, which increase with c_s . This apparent aggregation is particularly evident for 657-0.5, for which \bar{M}_w rises by a factor of two as c_s increases from 0.001 M to 0.100 M. The similarity in \bar{M}_w for 657-2 and 657-4 is probably a consequence of the fact that 657-4 turned out to be a considerably broader fraction than 657-2, due to difficulties in controlling exactly the proportion of the total material that precipitates in a given fraction.

Plots of $\langle s^2 \rangle_z^{1/2}$ versus $\log c_s$, in Figs 7 and 8 corroborate the occurrence of aggregation in 130-0.5 and 657-0.5 with increasing c_s , and there is some tendency for $\langle s^2 \rangle_z^{1/2}$ to increase with c_s for more highly degraded fractions as well. The intrinsic viscosities of the fractions (Tables 1 and 2) do not, however, mimic the increases in molecular dimensions with c_s suggested by the $\langle s^2 \rangle_z^{1/2}$ data. As with the unfractionated samples, $[\eta]$ is

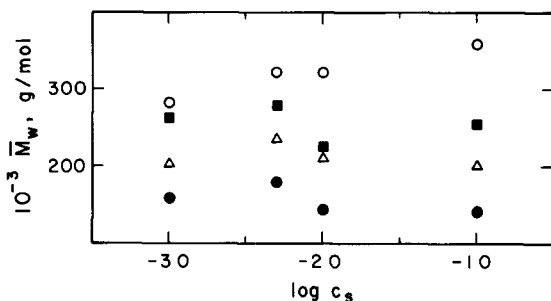


Fig. 5. Plots of \bar{M}_w versus $\log c_s$ for 130-0.5 (\circ), 130-1 (\blacksquare), 130-2 (\triangle) and 130-4 (\bullet) in aqueous NaCl.

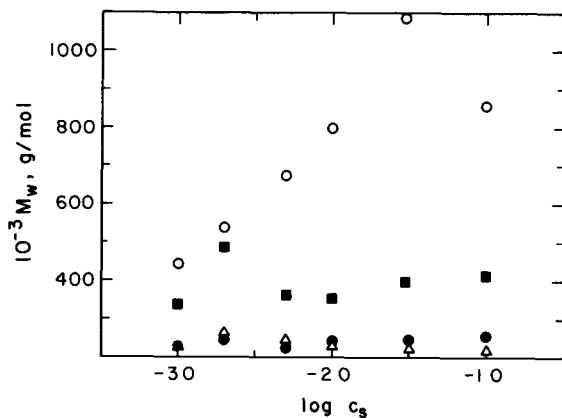


Fig. 6. Plots of \bar{M}_w versus $\log c_s$ for 657-0.5 (\circ), 657-1 (\blacksquare), 657-2 (\triangle) and 657-4 (\bullet) in aqueous NaCl.

sensibly independent of c_s for $c_s \geq 0.005$ M. At still lower c_s , $[\eta]$ is somewhat larger than the corresponding high-salt values, in contrast to what might initially be expected from the $\langle s^2 \rangle_z^{1/2}$ data. Aggregation leading to increases in $\langle s^2 \rangle_z^{1/2}$ but producing little or no change in $[\eta]$ can be rationalized readily (Tanner & Berry, 1974, Berry & Leach, 1981). Since $[\eta]$ measures the hydrodynamic volume per unit mass of polymer, aggregation of polymer coils in a way that retains within the polymer domain both the segment density and the extent of hydrodynamic interaction, i.e. 'draining', is expected to produce only minor changes in $[\eta]$ under conditions where $\langle s^2 \rangle_z^{1/2}$ increases perceptibly. Because in the present case the \bar{M}_w data disclose only a small extent of aggregation, even for 657-0.5, no inconsistency between the observed dependences of $\langle s^2 \rangle_z^{1/2}$ and $[\eta]$ on c_s is found.

Osmotic second virial coefficients determined by light scattering, A'_2 , decline with increasing salt concentration (Tables 1 and 2) as is expected for aqueous polyelectrolytes (Tanford, 1961). In surprising contrast to the salt dependence of $[\eta]$, however, A'_2 retains its salt sensitivity in the

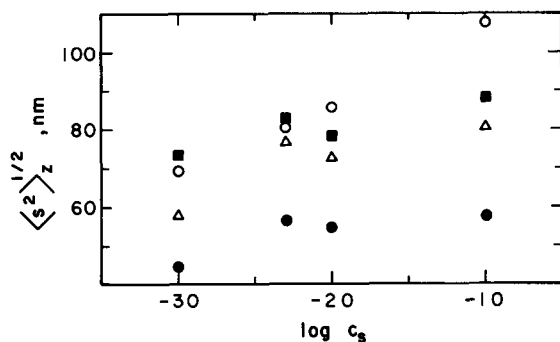


Fig. 7. Plots of $\langle s^2 \rangle_z^{1/2}$ versus $\log c_s$ for 130-0.5 (○), 130-1 (■), 130-2 (△) and 130-4 (●) in aqueous NaCl

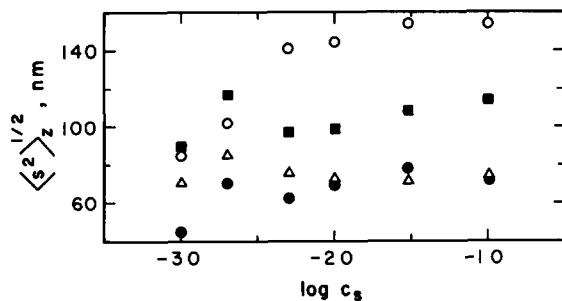


Fig. 8. Plots of $\langle s^2 \rangle_z^{1/2}$ versus $\log c_s$ for 657-0.5 (○), 657-1 (■), 657-2 (△) and 657-4 (●) in aqueous NaCl

concentration range $c_s > 0.005$ M. It is interesting to note that there is no systematic correlation between \bar{M}_w and the magnitude of A'_2 for either polymer. The explanation for this observation may reside in the complicated mix of factors contributing to A'_2 in polyelectrolyte systems (Hacche *et al.*, 1987). Thus, the relatively small A'_2 values displayed by 657-0.5 may reflect significant negative contributions from labile aggregation that responds by dissociation to dilution of the polymer in the light-scattering experiment. At $c_s = 0.1$ M, where the Donnan contributions to A'_2 are largely suppressed by the low molecular weight salt (Tanford, 1961), A'_2 is identical to within the experimental uncertainty for the four fractions of each polymer. Its magnitude at $c_s = 0.1$ M ($A'_2 = 1.2 \times 10^{-3}$ ml mol/g²) is, however, some three times larger than that of xanthan, a bacterial polysaccharide of similar composition and structure but with a greater linear charge density, at the same ionic strength (Paradossi & Brant, 1982, Hacche *et al.*, 1987).

Dependence on molecular weight

Correlations between various polymer observables and the molecular weight can often reveal useful information about the polymer chain configuration, a knowledge of the relationship of $[\eta]$ to \bar{M}_w can be of particular practical importance as well. Figure 9 displays the latter correlation for S-130 in the traditional logarithmic format, where the data for all four fractions at all four values of c_s are plotted together. The points fall into four different groups, each arranged approximately on a horizontal line corresponding to one of the S-130 fractions. There is little variation in vertical position within in a group, because of the minimal dependence of $[\eta]$ on c_s in the c_s range in question. If \bar{M}_w were also independent of c_s , each horizontal group would collapse to a single point. As seen in Fig. 5, most of the horizontal spread within each group can be attributed to the random error of the measurement of \bar{M}_w , and it is thus tempting to seek a numerical correlation of the data in Fig. 9, despite the fact that the range of \bar{M}_w values displayed covers less than half a decade. The linear least squares line shown in Fig. 9 was computed to fit only the data at $c_s = 0.1$ M. It is described by the Mark-Houwink equation $[\eta]_{0.1} = (3.37 \times 10^{-7}) M^{1.41}$. This line provides a reasonably good correlation of all of the data. Because \bar{M}_w increases most rapidly with decreasing sonication time at $c_s = 0.1$ M or, alternatively, because \bar{M}_w is most salt-dependent for the least degraded fractions (Fig. 5), the Mark-Houwink exponent for any other c_s than 0.1 M is even larger than that computed at $c_s = 0.1$ M. Thus, noting again the proviso already given about the narrow range of \bar{M}_w , S-130 appears to display the hydrodynamic behavior of a very stiff coil. Mark-Houwink exponents are typically in the range

0.8–1.0 for cellulose (Tanner & Berry, 1974), and approach 1.4 for the very stiff and presumably multistranded microbial polysaccharides xanthan and schizophyllan (scleroglucan) only in the range of \bar{M}_w below about 5×10^5 g/mol, where their behavior becomes nearly rodlike (Holzwarth, 1978; Yanaki *et al.*, 1980; Sato *et al.*, 1984).

The case for computing a numerical correlation of the S-657 $[\eta]$ versus \bar{M}_w data shown in Fig. 10 is less appealing, firstly, because the stronger dependence of \bar{M}_w on c_s for the least degraded fraction 657-0.5 obviates use of most of the \bar{M}_w data for this fraction and secondly, because fractions 657-2 and 657-4 are so similar in properties. The solid straight line in Fig. 10 is therefore obtained by the following alternative procedure. If, as may be postulated, the second side-chain sugar residue on S-657 has minimal additional influence on the backbone configuration of the polymer over and above the influence of the side-chain residue on S-130, then the principal difference in the Mark-Houwink plots for S-130 and S-657 should be a simple additive

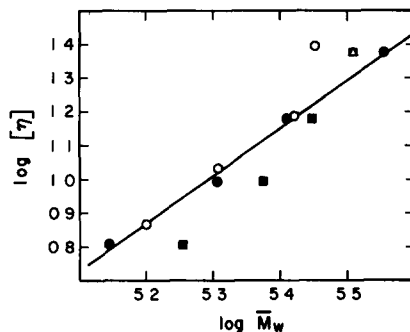


Fig. 9. Logarithmic plot of $[\eta]$ versus \bar{M}_w for S-130 fractions in aqueous NaCl at $c_s = 0.001$ M (\circ), 0.005 M (\blacksquare), 0.01 M (\triangle) and 0.1 M (\bullet) with a linear least squares regression line through the data at $c_s = 0.1$ M

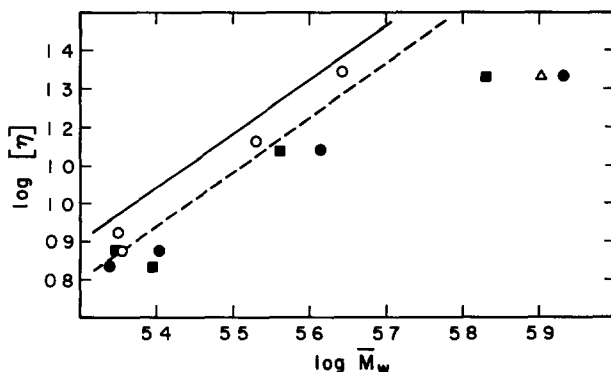


Fig. 10. Logarithmic plot of $[\eta]$ versus \bar{M}_w for S-657 fractions in aqueous NaCl at $c_s = 0.001$ M (\circ), 0.005 M (\blacksquare), 0.01 M (\triangle) and 0.1 M (\bullet). Lines drawn as described in the text

shift along the $\log \bar{M}_w$ axis to account for the difference in molar mass of the repeating unit. If the linear correlation of the S-130 data in Fig. 9 is subjected to a positive shift of $\log(6/5)$, where 6/5 represents the ratio of sugar residues in the nominal repeating units of S-657 and S-130, the solid line in Fig. 10 results. The additional shift of $\log(1.175)$ required to produce the dashed line in Fig. 10, which provides a plausible fit to all except the three suspect data points at highest \bar{M}_w , could well arise from the currently unknown differences in the extent of acylation of S-130 and S-657

If S-130 and S-657 are as stiff as suggested by the dependence of $[\eta]$ on \bar{M}_w , then $\langle s^2 \rangle_z^{1/2}$ should be approximately proportional to $(\bar{M}_z \cdot \bar{M}_{z+1})^{1/2}$ (Paradossi & Brant, 1982). Since no information on the molecular weight distributions of the fractions is available, one must be content to consider the dependence of $\langle s^2 \rangle_z^{1/2}$ on \bar{M}_w shown in Figs 11 and 12 for S-130 and S-657, respectively, in logarithmic plots. The straight lines through the data are linear least squares fits to all of the points, given for S-130 by $\langle s^2 \rangle_z^{1/2} = (2.30 \times 10^{-2}) \bar{M}_w^{0.65}$ and for S-657 by $\langle s^2 \rangle_z^{1/2} = (3.38 \times 10^{-2}) \bar{M}_w^{0.62}$. Rodlike chain behavior implies an exponent of unity,

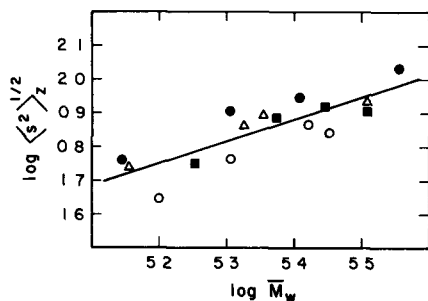


Fig. 11. Logarithmic plot of $\langle s^2 \rangle_z^{1/2}$ versus \bar{M}_w for S-130 fractions in aqueous NaCl at $c_s = 0.001$ M (\circ), 0.005 M (\blacksquare), 0.01 M (\triangle) and 0.1 M (\bullet) with a linear least squares regression line through all of the data

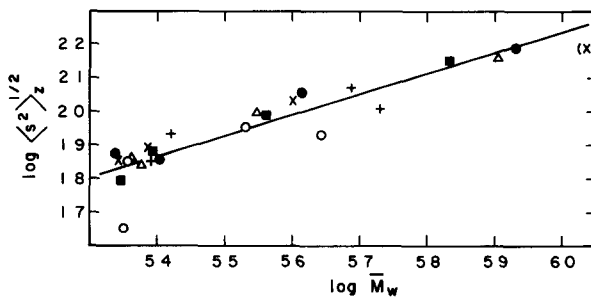


Fig. 12. Logarithmic plot of $\langle s^2 \rangle_z^{1/2}$ versus \bar{M}_w for S-657 fractions in aqueous NaCl at $c_s = 0.001$ M (\circ), 0.002 M ($+$), 0.005 M (\blacksquare), 0.01 M (\triangle), 0.03 M (\times) and 0.1 M (\bullet) with a linear least squares regression line through all of the data except the point at the largest \bar{M}_w

if the abscissa in Figs 11 and 12 is $\log(\bar{M}_z \cdot \bar{M}_{z+1})^{1/2}$, replacement of this quantity by $\log \bar{M}_w$ does not significantly change this expectation. Fits to the points corresponding to a given c_s yield in some cases somewhat larger exponents, although still less than one, and these are clearly no more reliable than the quoted values for the full data sets. Thus, one does not find in the apparent dependences of $\langle s^2 \rangle_z^{1/2}$ on \bar{M}_w support for very stiff chain behavior of S-130 and S-657, but these data are affected in an indeterminate way by the tendency of the samples to aggregate at higher salt concentrations and by uncertainties in the larger $\langle s^2 \rangle_z^{1/2}$ values occasioned by the limitation to scattering angles $\Theta > 30^\circ$ (Paradossi & Brant, 1982). It is interesting to observe that the logarithmic plots of $\langle s^2 \rangle_z^{1/2}$ versus \bar{M}_w for S-130 and S-657 nearly superimpose in the \bar{M}_w range in question, whereas one might expect, as with the $[\eta]$ versus \bar{M}_w data, to find the curve for S-657 shifted toward higher \bar{M}_w relative to that for S-130.

Polymer chain extension

For unperturbed random coils (signified by the subscript zero) the ratio $\langle s^2 \rangle_{0,z} / \bar{M}_z$ assumes an asymptotic value for large \bar{M}_z reflective of the mean polymer chain extension (Flory, 1953). Practical concerns dictate that the ratio of measurable properties $\langle s^2 \rangle_z / \bar{M}_w$ is often considered when θ -solvent data and information on sample polydispersity are not available. This quantity is reported for each fraction and salt concentration in Tables 1 and 2. Salt concentrations are confined to the range $c_s \geq 0.001$ M, for which there is little indication from $[\eta]$ and $\langle s^2 \rangle_z^{1/2}$ of declining polymer chain dimensions with increasing c_s . Contributions to a variation of $\langle s^2 \rangle_z / \bar{M}_w$ with c_s from polyelectrolyte effects thus appear to be minimal. Because both S-130 and S-657 are apparently quite extended chains (see below), it is also noted that for both polymers $\langle s^2 \rangle_z$ is probably a good approximation to $\langle s^2 \rangle_{0,z}$ (Tanner & Berry, 1974). Tanner & Berry (1974) argue that $\langle s^2 \rangle_z / \bar{M}_w$ should be relatively insensitive to small extents of aggregation. In the present case, however, the ratio shows a modest rise with increasing c_s , especially for S-130, where an increase of about a factor of 1.8 occurs over the range of c_s investigated. Thus, as might have been anticipated from Figs 5-8, the mean square radius of gyration displays a somewhat larger proportionate increase with c_s than does the molecular weight. Although one might anticipate non-asymptotic behavior of $\langle s^2 \rangle_z / \bar{M}_w$ for stiff polysaccharides in the lower range of molecular weights investigated here, the noise in the present measurements obscures any possible evidence of variation of $\langle s^2 \rangle_z / \bar{M}_w$ with \bar{M}_w . This factor serves also to mask possible differences in $\langle s^2 \rangle_z / \bar{M}_w$ arising from the differences in repeating unit weights for S-130 and S-657.

Of greatest interest is to compare the chain extension of S-130 and S-657 with other appropriate polymers, given the similarity of the backbone of the gellan family to cellulose and its derivatives, the comparison will be confined to the cellulose derivatives, including xanthan (Paradossi & Brant, 1982), and the soluble β -(1 \rightarrow 3, 1 \rightarrow 4)-barley glucan (Buliga *et al*, 1986). To eliminate the effect of differences in the molar masses of the repeating units, it is preferable to compare values of $\langle s^2 \rangle_z / \bar{x}'_w$, where \bar{x}'_w is the weight average number of backbone sugars in the chain. For polymers of the gellan family, \bar{x}'_w is four times the weight average degree of polymerization \bar{x}_w , and for xanthan \bar{x}'_w is twice \bar{x}_w . Comparisons are made in Table 3, where all of the entries except those for S-130, S-657, xanthan and the barley glucan are taken from the tabulation of Tanner & Berry (1974) with $\bar{x}'_w = \bar{x}_w$. Entries for S-130 and S-657 employ the average values of $\langle s^2 \rangle_z / \bar{M}_w$ from Tables 1 and 2, respectively, with conversion of \bar{M}_w to \bar{x}_w using the nominal repeating unit (equivalent) weights from the published structures omitting acyl substituents (Jansson *et al*, 1985, O'Neill *et al*, 1986, Chowdury *et al*, 1987). For xanthan, a repeating unit weight of 1000 g/mol was employed, and $\langle s^2 \rangle_z / \bar{M}_w$ was taken from the high molecular weight data of Paradossi & Brant (1982). The barley glucan is linear, so that $\bar{x}'_w = \bar{x}_w$, chain dimensions are estimated from Buliga *et al* (1986). Numbers in parenthesis in the cellulose derivative designations are the degrees of substitution (DS) of cellulose acetate (C(2.45)Ac), hexanoate (C(3.0)Hex), nitrate (C(2.90)N), and phenylcarbamate (C(3.0)PC). The quantity $\langle s^2 \rangle_z / \bar{x}'_w$ is reported in nm²/backbone sugar.

It appears from Table 3 that $\langle s^2 \rangle_z / \bar{x}'_w$ for both S-130 and S-657 is large relative to those for the barley glucan and many of the cellulose derivatives and, in fact, approaches that of the stiff, double-stranded microbial polysaccharide xanthan. Because of the considerable spread of $\langle s^2 \rangle_z / \bar{M}_w$ values in Tables 1 and 2, the mean values of $\langle s^2 \rangle_z / \bar{x}'_w$ for S-130 and S-657 in Table 3 cannot be considered different from one another. Moreover, they may also be larger than the true values because of aggregation, which affects $\langle s^2 \rangle_z$, especially at high c , and contributes to the reported means. On the other hand, inclusion of the acyl content of S-130 and S-657 in determining \bar{x}'_w would increase $\langle s^2 \rangle_z / \bar{M}_w$. (Mismatch of averages in the numerator (z-average) and denominator (w-average) may be quite significant for these relatively broadly dispersed fractions. Previous experience with xanthan, degraded and fractionated by similar procedures (Hacche *et al*, 1987), suggests that $\bar{M}_w / \bar{M}_n \approx 1.5$ for the present fractions. Assuming for simplicity of illustration a log-normal distribution for which $\bar{M}_z / \bar{M}_w = \bar{M}_w / \bar{M}_n$ (Elias *et al*, 1973), it is estimated that the values of $\langle s^2 \rangle_z / \bar{M}_w$ for S-130 and S-657 in Table 3 should be reduced by a factor of about 1.5 to account for polydispersity and yield

TABLE 3
Polymer Chain Extension

Polymer	$\langle s^2 \rangle_z / \bar{x}'_w$	Solvent
S-130	4.6	Aqueous NaCl (10^{-3} – 10^{-1} M)
S-657	5.5	Aqueous NaCl (10^{-3} – 10^{-1} M)
Xanthan	7.5	Aqueous NaCl (10^{-1} M)
Barley glucan	0.9	Water
C(2.45)Ac	2.35	Trifluoroethanol
C(2.45)Ac	2.35	Methylene chloride — methanol
C(3.0)Hex	1.80–2.50	1-Chloronaphthalene
C(3.0)Hex	2.10	Dimethylformamide
C(3.0)PC	2.60	Acetone
C(3.0)PC	4.70	Dioxane
C(3.0)PC	2.00	Dioxane — methanol
C(2.90)N	3.50	Acetone
C(2.90)N	5.40	Ethyl acetate

for S-130 and S-657 a composite value of $\langle s^2 \rangle_z / \bar{x}'_w$ of close to 3.3. Other data in Table 3 could be corrected similarly (Tanner & Berry, 1974), but the *relative* extensions of the several polymers would remain unchanged, and the authors will be content here to compare the uncorrected values of $\langle s^2 \rangle_z / \bar{x}'_w$.

Among the entries in Table 3, $\langle s^2 \rangle_z / \bar{x}'_w$ is least (0.9) for the β -(1 \rightarrow 3, 1 \rightarrow 4)-barley glucan. This polymer resembles cellulose with one-third to one-quarter of the β -(1 \rightarrow 4)-linkages replaced by isolated β -(1 \rightarrow 3)-linkages. The latter introduce points of departure from the highly extended and nearly rectilinear chain trajectories characteristic of the cellulosic backbone possessing unremitting β -(1 \rightarrow 4)-linkages (Buliga *et al.*, 1986). At the other end of the spectrum is xanthan for which $\langle s^2 \rangle_z / \bar{x}'_w = 7.5$ is some three times larger than that for C(2.45)Ac and several of the other synthetic cellulose esters. The large value for xanthan is almost certainly a consequence of the unusual stiffness afforded the chain by virtue of its double-stranded character in solution (Holzwarth, 1978; Paradossi & Brant, 1982; Sato *et al.*, 1984; Stokke *et al.*, 1988). Both S-130 and S-657 would appear structurally to mimic the barley glucan with an α -(1 \rightarrow 3)-linkage occurring at every fourth glycosidic junction in the backbone, whereas from the point of view of the magnitude of $\langle s^2 \rangle_z / \bar{x}'_w$ they more closely resemble xanthan.

The entries in Table 3 for C(3.0)PC in dioxane and C(2.90)N in acetone and ethyl acetate are also larger than those for the other synthetic derivatives of cellulose; they come, respectively, from the work

of Burchard (1965) and Huque *et al* (1958) Relatively large values of $\langle s^2 \rangle_z / \bar{x}'_w$ for high DS cellulose nitrate in acetone can also be deduced (Kamide *et al.*, 1979*a, b*) from the data of Schulz & Penzel (1968) and Penzel & Schulz (1968), while Holt *et al* (1976) report values of $\langle s^2 \rangle_z / \bar{x}'_w$ for high DS cellulose nitrate in ethyl acetate in the range 5–6 nm²/residue. The latter authors argue, in fact, that $\langle s^2 \rangle_z / \bar{x}'_w$ lies in this range for all cellulose derivatives and that smaller reported values, e.g. those for C(2.45)Ac in Table 3, have resulted from inadequate attention to the effect on the measured ratio from denser, aggregated components of the polymer sample This gel-like material presumably originates from the heterogeneous character of the reactions required to substitute the crystalline and generally insoluble cellulose Indeed, while the generalization of Holt *et al* (1976) may be too sweeping, many reports of $\langle s^2 \rangle_z / \bar{x}'_w$ for cellulose derivatives (Kamide & Miyazaki, 1978; Kamide *et al.*, 1979*a, b*, 1981) give values considerably smaller than the smallest of those compiled by Tanner & Berry (1974), for whom the experimental effects of aggregated material were of paramount concern The system C(3.0)PC/dioxane is perhaps the least problematic of all for reliable measurement of the solution properties of cellulose (Sutter & Burchard, 1979), and it has been implemented in procedures for routine determination of the molecular weight distribution of commercial cellulose samples (Cael *et al.*, 1981) The large value of $\langle s^2 \rangle_z / \bar{x}'_w$ for C(3.0)PC in dioxane must therefore be accorded considerable reliability This may, however, be a peculiarity of the particular system, arising from the bulkiness of the phenyl carbamate substituent groups and possible intramolecular hydrogen bond interactions among them (Sutter & Burchard, 1979), rather than a characteristic of all cellulose derivatives.

In view of the plentiful uncertainties remaining with regard to the chain extension of the cellulose derivatives, the authors are able to conclude only that the Kelco microbial polysaccharides S-130 and S-657 display a mean chain extension relative to the number of main-chain backbone residues that rivals the most extended of the synthetic cellulose derivatives, i.e. C(3.0)N in acetone or ethyl acetate and C(3.0)PC in dioxane, but probably does not quite mimic the extension of the double-stranded microbial cellulose derivative xanthan in 0.1 M aqueous NaCl This conclusion on the basis of the measured $\langle s^2 \rangle_z / \bar{x}'_w$ appears consistent with the large Mark-Houwink exponent reported above and obviates a reliable estimate of chain extension from the Flory-Fox equation (Jordan & Brant, 1980) Estimates of a persistence length for S-130 or S-657 using the molecular weight dependence of $[\eta]$ (Yamakawa & Yoshizaki, 1980) or $\langle s^2 \rangle_z$ (Benoit & Doty, 1953) are clearly premature, given the narrow molecular weight range studied

The large chain extension of S-130 and S-657 is perhaps surprising in view of the absence of any evidence to date for multistranded character of S-130 and S-657 in solution and the periodic interruptions of the extended β -(1 \rightarrow 4)-glucan linkage pattern that results from the α -(1 \rightarrow 3)-linkage between residues D and A (Fig 1) The structurally similar barley β -(1 \rightarrow 3, 1 \rightarrow 4)-glucans appear to support much less extended coils in dilute aqueous solution (Buliga *et al*, 1986), and preliminary modeling of the extension to be expected from single-stranded chains of the gellan family suggests values of $\langle s^2 \rangle / M$ for homogeneous samples of around unity (Talashek & Brant, 1987) in close agreement with the observed behavior of the barley glucan

CONCLUSIONS

Kelco microbial polysaccharides S-130 and S-657 have very similar dilute aqueous solution properties as might be anticipated from their common backbone repeating unit and the small differences in side chain structure Both display surprisingly weak polyelectrolyte character and have a similar, relatively large mean chain extension per backbone sugar residue which is comparable to that of the most highly extended synthetic cellulose derivatives but not so large as the double stranded microbial cellulose derivative, xanthan The large chain extension is interesting in view of the occurrence at every fourth backbone position of an α -(1 \rightarrow 3)-linkage, which might be expected to introduce directional variability into the otherwise essentially rectilinear and extended chain trajectories generated by the monotonous cellulosic backbone

ACKNOWLEDGEMENTS

This work has been supported by an unrestricted research grant from the Kelco Division of Merck, Inc, San Diego.

REFERENCES

- Bender, T M, Lewis, R J & Pecora, R (1986) *Macromolecules*, **19**, 244
Benoit, H & Doty, P (1953) *J Phys Chem*, **57**, 958
Berry, G C & Leech, M A (1981) In *Solution Properties of Polysaccharides*, ed D A Brant, ACS Symposium Series No 150, American Chemical Society, Washington, DC, p 61
Brownsey, G J, Chilvers, G R, l'Anson, K & Morris, V J (1984) *Int J Biol Macromol*, **6**, 211
Buliga, G S, Brant, D A & Fincher, G B (1986) *Carbohydr Res*, **157**, 139

- Buliga, G S & Brant, D A (1987) *Int J Biol Macromol* , **9**, 71
- Burchard, W (1965) *Makromol Chem* , **88**, 11
- Cael, J J, Cannon, R E & Diggs, A O (1981) In *Solution Properties of Polysaccharides*, ed D A Brant ACS Symposium Series No 150, American Chemical Society, Washington, DC, p 43
- Cesàro, A, Delben, F, Flaibani, A & Paoletti, S (1987) *Carbohydr Res* , **160**, 355
- Chandrasekaran, R, Millane, R P, Arnott, S & Atkins, E D T (1988) *Carbohydr Res* , **175**, 1
- Chowdhury, T A, Lindberg, B, Lindquist, U & Baird, J (1987) *Carbohydr Res* , **164**, 117
- Crescenzi, V, Dentini, M, Coviello, T & Rizzo, R (1986) *Carbohydr Res* , **149**, 425
- Crescenzi, V, Dentini, M & Dea, I C M (1987) *Carbohydr Res* , **160**, 283
- Dubin, P L & Brant, D A (1975) *Macromolecules*, **8**, 831
- Elias, H-G, Bareiss, R & Watterson, J G (1973) *Adv Polym Sci* , **11**, 111
- Flory, P J (1953) *Principles of Polymer Chemistry* Cornell University Press, Ithaca, NY, Chapter 14
- Goebel, K D & Brant, D A (1970) *Macromolecules*, **3**, 634
- Grasdalen, H & Smidsrød, O (1987) *Carbohydr Polym* , **7**, 371
- Hacche, L S, Washington, G E & Brant, D A (1987) *Macromolecules*, **20**, 2179
- Holt, C, Mackie, W & Sellen, D B (1976) *Polymer*, **17**, 1027
- Holzwarth, G (1978) *Carbohydr Res* , **66**, 173
- Huque, M M, Goring, D A I & Mason, S G (1958) *Can J Chem* , **36**, 952
- Jansson, P-E, Lindberg, B, Widmalm, G & Sandford, P A (1985) *Carbohydr Res* , **139**, 217
- Jordan, R C & Brant, D A (1980) *Macromolecules*, **13**, 491
- Kamide, K & Miyazaki, Y (1978) *Polym J* , **10**, 409
- Kamide, K, Terakawa, T & Miyazaki, Y (1979a) *Polym J* , **11**, 285
- Kamide, K, Miyazaki, Y & Abe, T (1979b) *Polym J* , **11**, 523
- Kamide, K, Saito, M & Abe, T (1981) *Polym J* , **13**, 421
- Moorhouse, R (1987) *Prog Biotechnol* , **3**, 187
- O'Neill, M A, Selvendran, R R, Morris, V J & Eagles, J (1986) *Carbohydr Res* , **147**, 295
- Paradossi, G & Brant, D A (1982) *Macromolecules*, **15**, 874
- Penzel, E & Schulz, G V (1968) *Makromol Chem* , **113**, 64
- Sanderson, G R (1988) In *Food Gels*, ed P Harris Elsevier, London, in press
- Sato, T, Kojima, S, Norisuye, T & Fujita, H (1984) *Polym J* , **16**, 423
- Schulz, G V & Penzel, E (1968) *Makromol Chem* , **112**, 260
- Smidsrød, O & Haug, A (1971) *Biopolymers*, **10**, 1213
- Stokke, B T, Smidsrød, O & Elgsaeter, A (1988) *Biopolymers*, **28**, 617
- Sutter, W & Burchard, W (1979) *Makromol Chem* , **179**, 1961
- Talashak, T A & Brant, D A (1987) *Carbohydr Res* , **160**, 303
- Tanford, C (1961) *Physical Chemistry of Macromolecules* John Wiley & Sons, NY, Chapter 4
- Tanner, D W & Berry, G C (1974) *J Polym Sci Polym Phys Ed* , **12**, 941
- Yamakawa, H & Yoshizaki, T (1980) *Macromolecules*, **13**, 633
- Yanaki, T, Norisuye, T & Fujita, H (1980) *Macromolecules*, **13**, 1462